

FDTD analysis of slow light propagation in negative-refractive-index metamaterial waveguides

To cite this article: E I Kirby *et al* 2009 *J. Opt. A: Pure Appl. Opt.* **11** 114027

View the [article online](#) for updates and enhancements.

Related content

- [Slow-light propagation in a cylindrical dielectric waveguide with metamaterial cladding](#)
Qi Zhang, Tian Jiang and Yijun Feng
- [Guided modes in negative-refractive-index fibres](#)
A V Novitsky and L M Barkovsky
- [Gyrotropic impact upon negatively refracting surfaces](#)
Allan Boardman, Neil King, Yuriy Rapoport *et al.*

Recent citations

- [Extended slow-light field enhancement in positive-index/negative-index heterostructures](#)
S. Foteinopoulou and J. P. Vigneron
- [Slowing light by exciting the fundamental degeneracy oscillatory mode in a negative refractive waveguide](#)
Tsung-Yu Huang *et al*
- [W. S. Wang *et al*](#)

FDTD analysis of slow light propagation in negative-refractive-index metamaterial waveguides

E I Kirby, J M Hamm, K L Tsakmakidis and O Hess

Advanced Technology Institute and Department of Physics, Faculty of Engineering and Physical Sciences, University of Surrey, Guildford GU2 7XH, UK

E-mail: O.Hess@surrey.ac.uk

Received 1 April 2009, accepted for publication 11 June 2009

Published 17 September 2009

Online at stacks.iop.org/JOptA/11/114027

Abstract

Using finite-difference time-domain (FDTD) simulations we investigate the propagation of light pulses in waveguides having a core made of a negative-refractive-index metamaterial. In order to validate our model we carry out separate simulations for a variety of waveguide core thickness. The numerical results not only qualitatively confirm that light pulses travel *slower* in waveguides with *thinner* cores, but further they reveal that the effective refractive indices experienced by the propagating pulses compare favourably with exact theoretical predictions. We also examine the propagation of light pulses in waveguides with adiabatically, longitudinally varying core refractive index. The effective refractive indices extracted from these simulations confirm previous theoretical predictions while, both a slowing and an increase in the amplitude of the pulses are observed.

Keywords: waveguides, negative-refractive-index, slow light

(Some figures in this article are in colour only in the electronic version)

1. Introduction

The ability to slow light opens up a wide range of potential applications, including ultracompact optical modulators and switches, enhanced optical nonlinearities, optical buffering and optical memory for quantum computers [1, 2]. The recently proposed idea of a ‘trapped rainbow’ by Tsakmakidis *et al* [3] illustrates how light pulses can be decelerated and stopped within a waveguide containing a negative-refractive-index (NRI) metamaterial [3]. Metamaterials have been under development for almost a decade now [4] and are composed of sub-wavelength artificial features, which through their interaction with light lead to the metamaterial exhibiting novel optical properties. Metamaterials having both a negative permittivity and a negative permeability have been experimentally constructed [4], tested and found to be in agreement with theory in frequency regions from the radio [5] all the way to the optical regime [6].

In recent years, extensive theoretical studies of the behaviour of lightwaves in waveguides composed of plasmonic [7–12] or NRI [13–20] materials have been carried out.

One of the novel features of such waveguides is the possibility of supporting forward and backward modes, which may be of the same order and exist simultaneously, in the same frequency region, inside the waveguide—but with different propagation characteristics. An advantage of the NRI structures as compared to their plasmonic (single-negative permittivity or permeability) counterparts is that they can facilitate (slow) light propagation for both polarizations (TM and TE); an attribute that can be important for certain applications, such as in modulators and switches [21].

The ‘trapped rainbow’ concept makes use of the fact that in a waveguide with an NRI core the cycle-averaged power flow in the core is oppositely directed to that within the positive refractive index (PRI) cladding material [3, 13–18]. This results in a *negative* Goos–Hänchen (GH) lateral displacement each time the ray is totally internally reflected as it propagates in a zigzag fashion along the waveguide, i.e. it is as if the ray travels three ‘steps’ forwards as it crosses the core and one ‘step’ back due to the negative GH lateral displacement [3], thus explaining why the light ray propagates slowly.

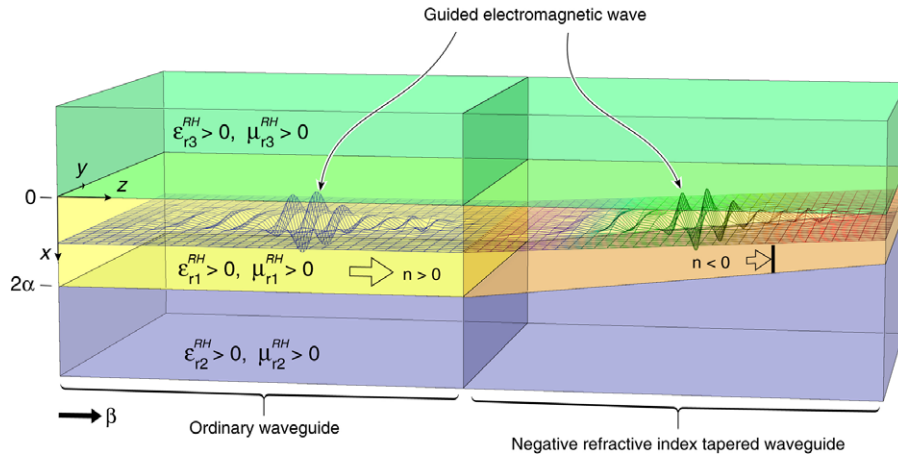


Figure 1. Schematic illustration of an oscillatory pulse guided along an ordinary dielectric waveguide and coupled to an adiabatically tapered NRI core waveguide. Each frequency component (‘colour’) of the pulse stops at a correspondingly different point inside the tapered negative-index waveguide, forming a ‘trapped rainbow’.

The authors of [3] envisioned slowing and stopping a light pulse by varying the thickness of the waveguide core to the point where the cycle-averaged power flow in the core and the cladding become comparable. At the degeneracy point, where the magnitudes of these powers become equal, the total time-averaged power flow directed along the central axis of the core vanishes. At this point the group (or energy) velocity goes to zero and the path of the light ray forms a double light cone (‘optical clepsydra’) where the negative GH lateral shift experienced by the ray is equal to its positive lateral displacement as it travels across the core [3]. Adiabatically reducing the thickness of the NRI core layer may, thus, in principle, enable complete trapping of a range of light rays, each corresponding to a different frequency contained within a guided wavepacket, as illustrated in figure 1.

The ‘trapped rainbow’ concept has previously been investigated through numerical simulations in a variety of waveguide structures [10–12, 19, 20]. A light pulse propagating along the waveguide was observed to slow down as the thickness of the core was reduced. In our present work, the effective refractive indices experienced by a light pulse for different NRI core thickness are computed and compared with analytically derived values. We then proceed with proposing a novel waveguide geometry where instead of varying the thickness of the core, we (adiabatically) vary the (negative) core refractive index and we investigate in detail the implications that such a variation has on the propagation of a light pulse along the waveguide.

2. Negative-refractive-index waveguide geometry

The system under investigation is a symmetric 2D waveguide (the permittivity and permeability of the cover and the substrate materials are equal). The substrate and cover are collectively referred to as the cladding. The core is composed of an isotropic NRI material, while the cladding contains a PRI material. Details of the geometric set up are shown in figure 2.

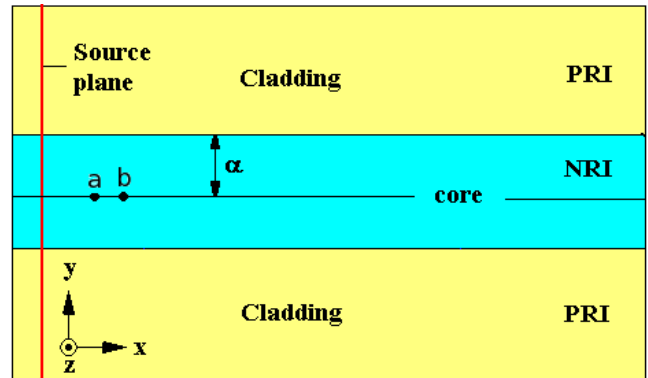


Figure 2. Waveguide geometry containing an NRI material core (pale blue) and PRI cladding (yellow). The source plane is where the input pulse is injected into the geometry, while a and b denote two measurement (recording) points along the central axis of the waveguide, and α is the half core thickness (figure not to scale).

3. Numerical model

Our full-wave numerical experiments were performed using the two-dimensional finite-difference time-domain (FDTD) method, which in the past has been shown to enable efficient and accurate simulations of NRI metamaterials [22]. Although the effective magnetic permeability in most magnetic metamaterials has, until now, exhibited a Lorentzian variation with frequency, here, for simplicity and in order to allow the core material to have an NRI over a broad range of frequencies, both the permittivity and the permeability response of the NRI material are modelled following a Drude material model. The permittivity and the permeability are modelled using the same plasma frequency; hence the dispersive refractive index of the NRI material [22] is given by:

$$n(\omega) = 1 - \frac{\omega_p^2}{\omega^2 + i\omega\Gamma}, \quad (1)$$

where ω_p is the plasma frequency and Γ the collision frequency. The material response is incorporated into the

program using the auxiliary differential equation (ADE) method [22–24]. In our simulations the cladding layers were purely dielectric, with a frequency independent permittivity equal to 1 (air).

For simplicity, in all the simulations presented in this paper, the materials are modelled as being lossless, i.e. with the collision frequency set to 0. It is to be noted, however, that none of the theoretical or numerical conclusions fundamentally change when dissipative losses are included in the analysis, so long as one considers (and numerically excites) guided light *pulses* having (in the presence of material losses) a *real* propagation constant and *complex* frequency [25, 31].

A modified total-field scattered-field (TFSF) formulation [24] combined with a suitable transverse field profile excitation was deployed in order to achieve single-mode launching. This methodology allowed us to excite and study individual waveguide modes even for frequency regions where both forward and backward modes coexisted. Special care was taken for the cladding material to be wide enough to ensure the amplitude of the evanescent field is sufficiently low at the boundaries of the computational domain, which were terminated by means of a uniaxially perfectly matched layer [24]. For the excitation of the input pulse we used two field components (H_z and E_y). The specification of the numerical wavevectors associated with these two components allowed us to stipulate the direction along which the initial pulse propagated inside the NRI waveguide. For all numerical experiments presented here, a time step of $dt = 0.706 dx/c$ has been used (c being the vacuum speed of light).

An oscillatory (fast) mode, whose field components oscillate within the core and exponentially decay inside the cladding, is used. The mode excited is the first-order even transverse magnetic (TM) mode, whose magnetic field is directed along the z axis, out of the plane of the 2D geometry. This mode has *two* nodal points inside the core, in the simulations the backward mode is used and so the excited mode is therefore defined as the TM_2^b mode as in [17].

4. NRI waveguides with different core thicknesses

A series of numerical experiments were conducted in order to analyse the effect that the thickness of the core has on the propagation of a light pulse along the NRI waveguide. Owing to the inherent scalability characterizing Maxwell’s equations of electromagnetism, all wavelengths and distances in this work are given as multiples of the cell length (grid units). Simulations of waveguides with core thicknesses (2α) of 82, 90, 100, 120 and 140 grid units were carried out. The free space wavelength of the central frequency (ω) of the pulse, used in each of these simulations, is 300 grid units. A fixed plasma frequency of $\omega_p = 2\omega$ is used to produce a refractive index of $n_{co} = -3$ in the core material at the centre frequency (ω). Both the rise and decay times of the Gaussian shaped pulse envelope are kept constant in order to ensure that the same range of frequencies is excited for each simulation run.

In these simulations we excited backward waves, since for the waveguide geometry implemented these modes can propagate in waveguides with a wider range of core

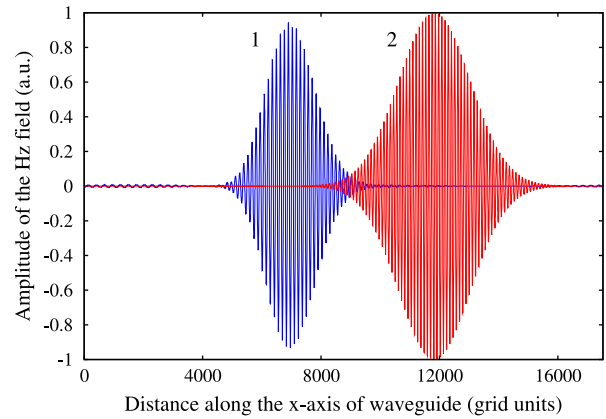


Figure 3. Snapshots of the H_z -field component along the central axis of the considered NRI waveguides. In both simulations the *same* time period has elapsed. The first pulse (blue, 1) corresponds to NRI waveguides with a thickness of 90 grid units, while for the second pulse (red, 2) the core thickness is 140 grid units.

thicknesses. Further, when an NRI material is used in the core, the backward modes are more strongly confined into the core, extending a shorter distance into the cladding than the corresponding forward modes. This allows for a thinner width of cladding material to be used, reducing the size of the computational domain required.

5. FDTD simulations of pulse propagation in NRI waveguides with different core thicknesses

Figure 3 shows a superposition of two snapshots of the H_z -field component along the central axis of the simulation geometry. The snapshots show one pulse (blue, 1) propagating inside an NRI waveguide with a core thickness of 90 grid units, and a second pulse (red, 2) propagating along an NRI waveguide with a core thickness of 140 grid units. The two snapshots are recorded after the *same* time interval from the start of each simulation. The pulses travel from left to right. One may directly infer from figure 3 that the pulse in the waveguide with the thinner core travelled a shorter distance compared to the pulse in the thicker waveguide during the considered time period. This difference exists even though both pulses experience the same refractive index of the core material.

With the present time-domain simulation approach one may readily calculate the effective refractive index experienced by individual frequencies in the pulse [23, 24, 26, 27], and then compare it with corresponding analytical results. Two recording points a and b are placed along the central axis of the waveguide (see figure 2) at which the H_z -field values are recorded over time. One may then Fourier transform the output at each point and calculate the dependence of the longitudinal propagation constant (β) on frequency.

The (real) effective index ($n_{\text{eff}} = \beta/k_0$) at the frequency of interest can then be extracted as:

$$n_{\text{eff}} = \frac{1}{k_0 d} (\varphi|_b^{f_0} - \varphi|_a^{f_0}), \quad (2)$$

where $\varphi|_a^{f_0}$ and $\varphi|_b^{f_0}$ are the phase of the frequency of interest (f_0) at points a and b , k_0 the free space wavevector of the

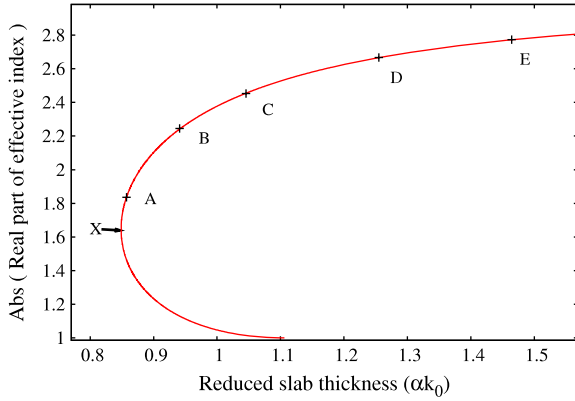


Figure 4. Comparison between numerical (black points) and analytical (solid red) results concerning the effective refractive index of the TM_2 mode, propagating along the NRI waveguide of figure 2. In the FDTD simulations, the core thicknesses (2α) in grid units were, respectively: 82 (point A), 90 (point B), 100 (point C), 120 (point D), and 140 (point E). X marks the degeneracy point; the region of the curve with effective index values greater than that of the degeneracy point is where backward modes are able to exist, while forward modes exist in the region with smaller effective index values.

frequency of interest and d the separation of the two recording points.

In these simulations the wavelength (*inside* the waveguide) corresponding to the frequency of interest should be larger than the distance between the two recording points (a and b) to ensure that the wave phase difference between the two points is smaller than 2π . If the wavelength is smaller than the distance between the measurement points, the measured phase difference will require an additional factor of $2n\pi$ added to it (with n being a positive integer), which may be unknown.

In our computations we observed that the effective phase index was *negative*, indicating that the phase was directed backwards, towards the source. Indeed, as expected for a backward mode, the direction of the phase velocity is opposite to the direction of the group or energy velocity, and as a result the pulse propagates (with its *positive* group velocity) causally, *away* from the source.

To facilitate direct comparison with an analytically calculated geometric-dispersion diagram, where the effective index is taken to be positive, we take the absolute value of the effective indices obtained from the simulations. This allows the effective index extracted from each simulation (and corresponding to a frequency closest to the central frequency of the numerical pulse) to be plotted (overlaid) on the theoretical geometric-dispersion diagram. The analytic geometric-dispersion curve for even TM modes in lossless waveguides can be calculated using equation (3), which is derived from Maxwell's equations and the boundary conditions for the transverse fields [28]:

$$\alpha k_0 = \frac{1}{(\epsilon_{co}\mu_{co} - n_{eff}^2)^{\frac{1}{2}}} \times \left[\arctan \left(\frac{\epsilon_{co}(n_{eff}^2 - \epsilon_{cl}\mu_{cl})^{\frac{1}{2}}}{\epsilon_{cl}(\epsilon_{co}\mu_{co} - n_{eff}^2)^{\frac{1}{2}}} \right) + m\pi \right], \quad (3)$$

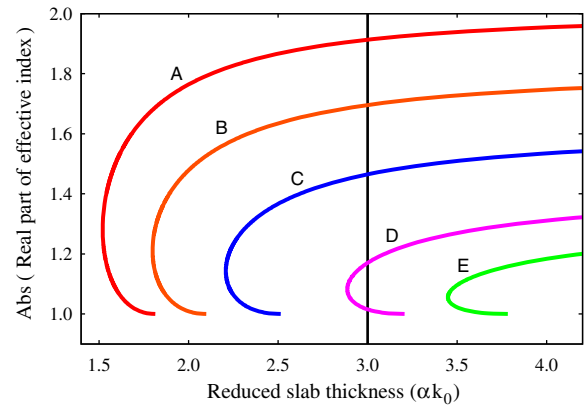


Figure 5. Geometric dispersion diagrams for waveguides with a core refractive index n_{co} equal to: (A) -2 , (B) -1.8 , (C) -1.6 , (D) -1.4 , and (E) -1.3 . The refractive index of the cladding is constant at $n_{cl} = 1$.

n_{eff} being the effective index experienced by the pulse, m the order of the mode, while ϵ_{co} , μ_{co} and ϵ_{cl} , μ_{cl} are the relative permittivity and permeability of the core and cladding layers, respectively. Note that in the geometric-dispersion diagram the variation of the reduced slab thickness is performed only via changing the core thickness (α), i.e. a constant frequency is used, since the values of ϵ_{co} and μ_{co} used in equation (3) are frequency dependent.

Figure 4 reports the so-extracted real part of the effective indices of the first-order even mode for various core thicknesses (black points), as well as the corresponding analytically derived dispersion curve (solid red). Note the excellent agreement between the numerical and analytical results for a range of waveguide thicknesses, which confirms the accuracy in the single-mode excitation and extraction of the mode effective index.

6. Including a refractive index gradient in the core

The ‘trapped rainbow’ concept envisions an adiabatic reduction in the width of the core layer along the longitudinal direction of the metamaterial waveguide (see figure 1). This is predicted to decelerate a polychromatic pulse, eventually ‘trapping’ it in a finite space region such that each frequency component of the pulse stops at a different position along the waveguide.

Accurate modelling of a waveguide with an axially varying metamaterial core thickness can be challenging owing to a well-known difficulty in the numerical description of media interfaces, especially when metamaterials are involved [29, 30]. To mitigate this numerical difficulty, here we studied a modified (but fully equivalent) waveguide geometry, wherein the thickness of the NRI core layer is kept *constant* and the refractive index of the core material is smoothly (adiabatically) varied in the longitudinal direction. Figure 5 demonstrates how a suitable variation of the core refractive index leads to an alteration in the shape of the dispersion curve and a change in the propagation constant as observed for a particular value of the reduced slab thickness; at a

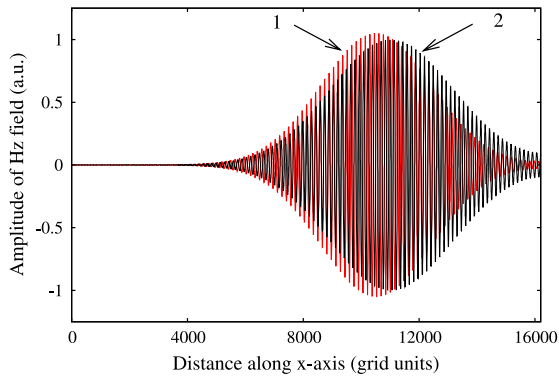


Figure 6. Snapshots from the propagation of the H_z -field component along the central axis of a waveguide with an axially varying core refractive index (red; 1) and a waveguide with a uniform core refractive index (black; 2).

particular value of the core refractive index the degeneracy point coincides with this core thickness. For instance, inspection of figure 5 reveals a situation where, for a reduced slab thickness of $\alpha k_0 = 3$, a sinusoidal wave propagating along a waveguide with an initial core refractive index of $n_{co} = -2$ (red line, A) would be cut off *before* the refractive index value was increased to $n_{co} = -1.3$ (green line, E).

7. FDTD modelling of light propagation in NRI waveguides with adiabatically varied core refractive index

To test the effect that a variation of the core refractive index along the longitudinal axis has on the propagation of a guided lightwave, we performed a similar numerical experiment to those presented in section 5, with the thickness of the core layer kept constant throughout the waveguide structure. The central frequency of the numerical pulse corresponded to a free space wavelength of 200 grid units, while the core thickness was kept constant at 190 grid units. A plasma frequency of $\omega_p = (\sqrt{2.5})\omega$ resulted in a core refractive index (at the central frequency of the pulse) of $n_{co} = -1.5$. The refractive index of the core material was spatially adiabatically varied by suitably adjusting the plasma frequency along the longitudinal axis of the waveguide. The gradient of the plasma frequency was chosen so as to produce a linear variation in the core refractive index. Particular care has been taken to ensure that the cut off points for each of the frequencies excited in the pulse are not reached, allowing the propagation of the pulse to be shown clearly.

Figure 6 reports a comparison between a pulse (shown in red, 1) in an NRI waveguide, the core of which has an axially varying refractive index (VRI) (in this case from $n_{co} = -1.5$ to -1.44 over 16000 grid units) and a pulse (shown in black, 2) in an NRI waveguide with a uniform refractive index of $n_{co} = -1.5$ (which is the initial refractive index of the core in the VRI waveguide). Shown in figure 6 is the H_z -field component recorded along the central axis of the two simulations and at the same time point. Again both pulses propagate from left to right, it can be seen that the pulse in the VRI waveguide

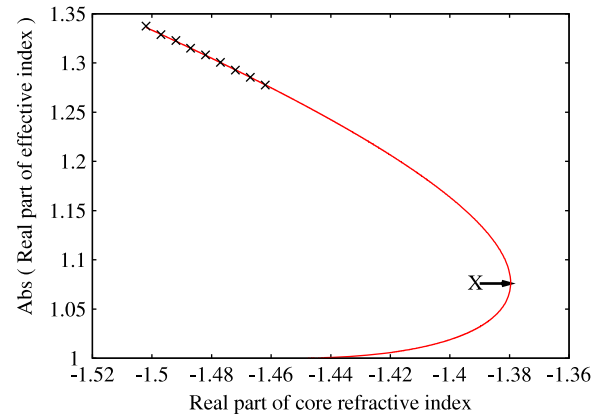


Figure 7. Variation of the TM_2 mode effective index with the refractive index of the core for a constant thickness of the core layer. Black points—results from FDTD simulation; Red solid line—theoretical prediction. Again, X shows the degeneracy point.

travels a shorter distance as compared to the pulse propagating inside the uniform refractive index waveguide. Inspection of figure 6 also shows that the amplitude of the pulse in the VRI waveguide has increased from its initial value of unity. This relates to the fact that at any moment in time the rear of the pulse inside the VRI waveguide travels faster than the front of the pulse. In catching up to the front, the length of the pulse is thereby reduced, i.e. the pulse is spatially compressed, and its amplitude increases. Such an effect was also observed, e.g. in [19, 20], where the thickness of the core was reduced along the waveguide.

To track the change in the propagation constant of the pulse as it travels along the VRI waveguide we recorded the H_z -field components at several points along the central axis of this waveguide. A theoretical prediction for the progressive change in the effective index that the measured frequency experiences as it propagates down the waveguide is made by making a suitable modification to equation (3), whereby the αk_0 value is kept constant (denoting a constant core thickness and central pulse frequency) while the effective index is calculated for different values of the core refractive index. The effective indices obtained from the FDTD simulation results for the measured frequency (which is close to the central frequency of the pulse) at different points along the VRI core are plotted in figure 7, together with the theoretically predicted results (for the same frequency).

Similarly to figure 4, we observe a very good agreement between the analytically calculated and numerically computed results. As can be seen from figure 7, if the maximum refractive index of the taper was extended from $n_{co} = -1.44$ to -1.38 , the degeneracy point for the measured frequency, where the energy in the core and cladding cancel, producing a zero energy velocity, would have also been reached.

8. Conclusions

In summary, using full-wave FDTD simulations we have shown that the core thickness of an NRI waveguide has a pronounced effect on, both, the energy velocity and the phase

index of a guided lightwave. A comparison was made between the simulation and analytically calculated results concerning the effective refractive index of a guided lightwave, and our results demonstrated good agreement between the two.

We have further investigated the effect that the adiabatic variation of the negative refractive index of the core layer has on the speed of the guided light. It was concluded that increasing the core index is similar in effect to reducing the width of the core, in that the energy velocity of the pulse is reduced and the amplitude of a guided pulse increases when compared to a pulse propagating inside a uniform-refractive-index core waveguide, where the core refractive index is the same as that at the start of the varying-refractive-index (VRI) metamaterial waveguide. We have further shown that the variation of the effective index of a pulse travelling along a varying-refractive-index (VRI) metamaterial waveguide agrees well with theory.

Acknowledgments

This work was supported by the UK Engineering and Physical Sciences Research Council (EPSRC). K L Tsakmakidis acknowledges support by the Royal Academy of Engineering and the EPSRC through a research fellowship.

References

- [1] Mok J T and Eggleton B J 2005 Expect more delays *Nature* **433** 811–2
- [2] Krauss T F 2008 Why do we need slow light? *Nat. Photon.* **2** 448–50
- [3] Tsakmakidis K L, Boardman A D and Hess O 2007 ‘Trapped rainbow’ storage of light in metamaterials *Nature* **450** 06285
- [4] Smith D R, Padilla W J, Vier D C, Nemat-Nasser S C and Schultz S 2000 Composite medium with simultaneously negative permeability and permittivity *Phys. Rev. Lett.* **84** 4184–7
- [5] Wiltshire M C K, Pendry J B, Young I R, Larkman D J, Gilderdale D J and Hajnal J V 2001 Microstructured magnetic materials for RF flux guides in magnetic resonance imaging *Science* **291** 849–51
- [6] Dolling G, Wegener M, Soukoulis C M and Linden S 2007 Negative-index metamaterial at 780 nm wavelength *Opt. Lett.* **32** 53–5
- [7] Alù A and Engheta N 2004 Guided modes in a waveguide filled with a pair of single-negative (SNG), double-negative (DNG), and/or double-positive (DPS) layers *IEEE Trans. Microw. Theory Tech.* **52** 199–210
- [8] Alù A and Engheta N 2005 An overview of salient properties of planar guided-wave structures with double-negative (DNG) and single-negative (SNG) layers *Negative Refraction Metamaterials: Fundamental Properties and Applications* ed G V Eleftheriades and K G Balmain (Hoboken, NJ: IEEE, Wiley) chapter 9, pp 339–80
- [9] Alù A and Engheta N 2006 Optical nanotransmission lines: synthesis of planar left-handed metamaterials in the infrared and visible regimes *J. Opt. Soc. Am. B* **23** 571–583
- [10] Gan Q, Fu Z, Ding Y J and Bartoli F J 2008 Ultrawide-bandwidth slow-light system based on THz plasmonic graded metallic grating structures *Phys. Rev. Lett.* **100** 256803
- [11] Fu Z, Gan Q, Ding Y J and Bartoli F J 2008 From waveguiding to spatial localization of THz waves within a plasmonic metallic grating *IEEE J. Sel. Top. Quantum Electron.* **14** 486–90
- [12] Gan Q, Ding Y J and Bartoli F J 2009 ‘Rainbow’ trapping and releasing at telecommunication wavelengths *Phys. Rev. Lett.* **102** 056801
- [13] Shadrivov I V, Sukhorukov A A and Kivshar Y S 2003 Guided modes in negative-refractive-index waveguides *Phys. Rev. E* **67** 057602
- [14] Nefedov I S and Tretyakov S A 2003 Waveguide containing a backward-wave slab *Radio Sci.* **38** 1101–9
- [15] Peacock A C and Broderick N G R 2003 Guided modes in channel waveguides with a negative index of refraction *Opt. Express* **11** 2502–10
- [16] He J and He S 2005 Slow propagation of electromagnetic waves in a dielectric slab waveguide with a left-handed material substrate *IEEE Microw. Wirel. Compon. Lett.* **16** 96–8
- [17] Tsakmakidis K L, Klaedtke A, Aryal D P, Jamois C and Hess O 2006 Single-mode operation in the slow-light regime using oscillatory waves in generalized left-handed heterostructures *Appl. Phys. Lett.* **89** 201103
- [18] Alekseyev L V and Narimanov E 2006 Slow light and 3D imaging with non-magnetic negative index systems *Opt. Express* **14** 11184–93
- [19] He J, Jin Y, Hong Z and He S 2008 Slow light in a dielectric waveguide with negative-refractive-index photonic crystal cladding *Opt. Express* **16** 11077–82
- [20] Jiang T, Zhao J and Feng Y 2009 Stopping light by an air waveguide with anisotropic metamaterial cladding *Opt. Express* **17** 170–7
- [21] Gardes F Y, Tsakmakidis K L, Thompson D, Reed G T, Mashanovich G Z, Hess O and Avitabile D 2007 Micrometer size depletion-type photonic modulator in silicon on insulator *Opt. Express* **15** 5879–84
- [22] Ziolkowski R W 2003 Pulsed and CW Gaussian beam interactions with double negative metamaterial slabs *Opt. Express* **11** 662–81
- [23] Ziolkowski R W and Heyman E 2001 Wave propagation in media having negative permittivity and permeability *Phys. Rev. E* **64** 056625
- [24] Taflove A and Hagness S C 2005 *Computational Electrodynamics: the Finite-Difference Time-Domain Method* 3rd edn (Norwood, MA: Artech House Publishers)
- [25] Huang K C, Lidorikis E, Jiang X, Joannopoulos J D, Nelson K A, Bienstman P and Fan S 2004 Nature of lossy Bloch states in polaritonic photonic crystals *Phys. Rev. B* **69** 195111
- [26] Tsakmakidis K L, Hermann C, Klaedtke A, Jamois C and Hess O 2005 Systematic modal analysis of 3D dielectric waveguides using conventional and high accuracy nonstandard FDTD algorithms *IEEE Photon. Technol. Lett.* **17** 2598–600
- [27] Tsakmakidis K, Weiss B and Hess O 2006 Full-wave electromagnetic modelling of an InP/InGaAs travelling-wave heterojunction phototransistor *J. Phys. D: Appl. Phys.* **39** 1805–14
- [28] Cherin A H 1983 *An Introduction to Optical Fibers* (Japan: McGraw-Hill) pp 63–4
- [29] Zhao Y, Belov P and Hao Y 2007 Accurate modelling of left-handed metamaterials using a finite-difference time-domain method with spatial averaging at the boundaries *J. Opt. A: Pure Appl. Opt.* **9** S468–75
- [30] Zhao Y, Belov P and Hao Y 2007 Accurate modelling of the optical properties of left-handed media using a finite-difference time-domain method *Phys. Rev. E* **75** 037602
- [31] Archambault A, Teperik T V, Marquier F and Greffet J J 2009 Surface plasmon Fourier optics *Phys. Rev. B* **79** 195414